Study on machining performance in grinding of Ni-base single crystal superalloy DD5

Ming Cai
Tao Zhu
Xingjun Gao (gxj7976@126.com)
Liaoning Petrochemical University
Yongfei Yan
Ning Yu
Lei Zeng

Research Article

Keywords: Surface integrity, Chip morphology, Ni-base single crystal superalloy DD5, Grinding force, MQL

Posted Date: February 16th, 2022

DOI: https://doi.org/10.21203/rs.3.rs-1335303/v1

Abstract

The Ni-base single crystal superalloy DD5 is commonly employed in critical parts of turbine blades and turbine discs in aeronautical engines. To improve the surface machining quality, single-factor experiments were carried out to investigate the changes of grinding force, surface morphology and chip morphology under different grinding conditions (dry, conventional flood, minimum quantity lubrication). The experiments showed that the conventional flood lubrication and minimum quantity lubrication (MQL) could enormously reduce the surface roughness, grinding force, and work-hardened layer thickness of DD5. At the depth of 5~15 μm, the DD5 subsurface microhardness decreased sharply with the increase of depth, and the microhardness under different grinding conditions was in the order of dry grinding, conventional flood, and MQL. However, at the depth of 20~150 μm, the DD5 subsurface microhardness tended to equilibrate and fluctuate around 540 HV. In addition, compared with dry grinding, the degree of chip serration was obvious in flood or MQL environment, and its chip formation frequency fluctuated less and chip formation was stable. Within the experimental parameters, the MQL grinding machining method obtained the lowest surface roughness and the highest surface quality with the lowest associated cost, which is the ideal grinding and cooling lubrication method for the Ni-base single crystal superalloy.

1 Introduction

Ni-base superalloys, with excellent high-temperature strength and corrosion resistance, can work reliably for a long time with high stability and have been widely used in the most severe working conditions such as turbine guide vanes and combustion vortex chamber parts of aero-engines. At present, the most promising Ni-base superalloys for aero-engines are Ni-base polycrystalline superalloys and Ni-base single crystal superalloys. Compared with Ni-base polycrystalline superalloys, single crystal superalloys have reduced grain boundary strengthening elements (B, Zr, C, Hf, etc.) and eliminated grain transverse grain boundaries, which are prone to cracking sources, making Ni-base single crystal superalloys significantly more resistant to high temperature and creep. The grinding process, as an important manufacturing method for Ni-base single crystal superalloys, can obtain lower surface roughness and better surface quality.

However, the excellent mechanical qualities of Ni-base superalloys can lead to grinding process drawbacks such as high grinding temperatures, limited grinding wheel life, and poor machined surface quality.[1]. To solve those problems, experimental studies on the grinding process characteristics of Ni-base superalloys have been studied by researchers. Zhou et al. [2] investigated the effects of grinding speed, grinding wheel feed rate and grinding depth on the DD98 roughness of Ni-base single crystal superalloys by the response surface method. When grinding DZ408, K403, and GH4169 with alumina grinding wheels, Miao et al. [3] discovered that abrasive wear and material adhesion occurred mostly on the grinding wheels, whereas DD6 was blocked on the grinding wheels. Cai et al. [4–5] conducted an orthogonal experiment on the grinding surface quality of DD5, the study showed that the optimum surface quality was obtained when the angle θ was 45°. Ding et al. [6] effectively predicted the grinding surface topography by reconstructing the measured surface topography of CBN grinding wheels. Li et al.

[7] compared the tool wear behavior of microcrystalline Al_2O_3 grinding wheels with brown Al_2O_3 grinding wheels during grinding FGH96. In addition, the prediction of grinding forces when grinding FGH96 with electroplated CBN was performed [8]. In the study of the impact of abrasive wear on grinding surface properties and corrosion performance of K444 alloy, Li et al. [9] discovered that microcrystalline Al_2O_3 wheels had less abrasive wear and more excellent self-sharpening than white Al_2O_3 wheels. Ruzzi et al. [10] assessed the effect of several grinding parameters on the surface profile of Inconel 718. Zhao et al. [11] investigated the specific grinding energy and grinding heat flow during the leaf root formation grinding of DZ125 superalloy turbine blades. The study studied not only the temperature distribution on the machined surface and depth-of-cut direction but also the impact of heat source geometry and contact length on the temperature distribution. Gong et al. [12] created a model to predict the normal and tangential forces of a Ni-base single crystal superalloy and investigated the impact of cutting parameters on grinding force, grinding surface, and subsurface. Tian et al. [13] used the single-grain experiment technique to explore the impact of grinding speed on the surface profile of Ni-base single crystal superalloy. The single abrasive grain experiment technique was carried out to research the effect of grinding speed on the material removal of Ni-base superalloy GH4169, and the crucial chip formation thickness for chip formation was evaluated. Öpöz and Chen. [14–16] looked at the material removal process of single abrasive grinding, it was found that single-edge scratches were removed more efficiently, while multi-edge scratches were more likely to plow.

Adding a minimum quantity of lubricant to the grinding process has also become a green and efficient manufacturing method, it can reduce the use of lubricating fluid, keep costs down, and protect the environment while improving the surface finish of the workpiece. The vegetable oil-based nanofluid technology can form a stable lubricating film at the workpiece-tool interface, which boosts the roughness, G-ratio, and grinding specific performance of Inconel 718 [17]. Yazid et al. [18] found that dry cutting produced higher microhardness and more severe surface damage than MQL in the research of the surface integrity of Ni-base superalloy GH4169 under MQL cooling conditions. By studying the impact of MQL on cutting residual stress, He et al. [19] found that cooling and lubrication play a leading role in the cutting process. MQL mainly affects the generation of residual stress by affecting the thermal effect. Enhancing the cooling performance of MQL can reduce the residual tensile stress and obtain the residual compressive stress. Li et al. [20] explored the effect of lubrication conditions on the surface integrity of GH4169 under MQL cooling conditions and found that dry cutting produced higher microhardness and more severe surface damage than MQL. In contrast, Silva et al. [21] found little change in subsurface microstructure and no significant difference in probing the surface integrity of the material under different cooling conditions. Balan et al. [22] found that low-temperature MQL-assisted grinding with 50 ~ 65% lower cutting energy than conventional dry grinding could improve the processability of Inconel 751. Many researchers have reviewed sustainable machining of superalloy materials while outlining the latest trends and requirements [23–25]. Jia et al. [26] proposed a new method of gas-assisted electrostatic atomized minimum quantity lubrication and found that electrostatic atomized minimum quantity lubrication could significantly enhance the processing quality of Ni-base superalloy GH4169 compared to pneumatic atomized minimum quantity lubrication. Gong et al. [27] carried out a comparative grinding

experiment on Ni-base superalloy DD5 under MQL lubrication and dry grinding conditions and investigated the effect of thickness of the DD5 grinding metamorphic layer under cooling conditions. The study showed that the thickness of the metamorphic layer tended to decrease and then increase with the grinding speed, increase with the grinding depth, and increase and then decrease with the workpiece feed speed. And compared with dry grinding, MQL could reduce the thickness of the metamorphic layer by about 2.4–3.5 μm. Wang et al. [28] compared the thickness of the metamorphic layer of seven vegetable oils (soybean oil, peanut oil, palm oil, castor oil, corn oil, rapeseed, and sunflower oil) and liquid paraffin oil for MQL performance, and found that the processed surface quality of different base oils after trace lubrication was from superior to inferior in the following order: castor oil, palm oil, peanut oil, sunflower oil, soybean oil, rapeseed oil, and corn oil. Where, Guo et al. [29] found that the combined lubrication performance of the blended oils was better than that of castor oil, and the best lubrication performance was obtained with soybean/castor oil.

Some research results on the grinding process of Ni-base single crystal superalloys have been carried out by scholars. However, there have been few studies on the impact of varied cooling conditions on the grinding surface integrity of Ni-base single crystal superalloys. Therefore, the grinding process of Ni-base single crystal superalloy DD5 under different cooling conditions was conducted to explore the influence of grinding conditions on grinding force, surface roughness, surface morphology, chip morphology, microhardness of DD5.

2 Mechanism Of Minimum Quantity Lubrication

MQL is a technique of forming two-phase flow by mixing atomizing a small amount of lubricant with high-pressure gas, spraying it into the grinding region, and cooling it [30]. The atomized lubricating fluid and the high-pressure gas flow (0.4 ~ 0.65MPa) can effectively break the boundary layer of air in the grinding area and enter the grinding area for lubrication and cooling (as shown in Fig. 1). The high-pressure airflow constitutes convective heat exchange with the gas environment in the grinding area to reduce the grinding temperature. In addition, the high-pressure airflow carries away the generated grinding chips to prevent material coating or grinding wheel clogging, etc. What is more, the atomized lubricating fluid enters the grinding area to form an oil film, which reduces the coefficient of friction, thereby reducing grinding forces and grinding heat.

In the grinding process, there are four assumptions about the penetration mechanism of lubricating fluid: The suction phenomenon caused by grinding wheel vibration. (Fig. 2a); The diffusion penetration of the first deformation zone is shown in (Fig. 2b); The capillary network penetration (Fig. 2c); The cutting tumor periodically falls off and causes cavities (Fig. 2d). At present, capillary network penetration is generally considered to be the primary mechanism of lubricant penetration.

The material on the contact surface of debris abrasive grain machined surface has plastic deformation due to solid shear force, tensile and compressive stress and friction, resulting in microcracks on the contact surface of the material. Furthermore, the abrasive grains are not evenly distributed on the

grinding wheel, and the local hard spot plough on the abrasive grains produces micro-valleys on the workpiece surface. These micro-cracks and micro-valleys form capillaries, which are in a high-temperature and low-pressure environment, and quickly fill with lubricating fluid under the action of pressure difference.

3 Experiment

3.1 Experimental equipment

The experimental equipment in this paper is shown in Fig. 3. The grinding machine used for the experiment is the M7120A surface grinding machine, which has a maximum size of 630 mm × 200 mm × 320 mm and is mainly used for the relevant dry grinding or wet grinding tests. The table uses a hydraulic system with step-less speed control movement. Since the spindle speed of the surface grinding machine is constant, to investigate the influence law of the grinding wheel's linear speed on the grinding process, a Proton BT500 intelligent vector universal frequency converter is used to regulate the spindle speed of the surface grinding machine. The grinding wheel is made of CBN abrasive with good self-sharpening and sufficient toughness, with the code 80/100 (average particle size of 180 μm), medium-hard hardness, resin bond, 180 mm grinding wheel diameter, 32 mm mounting diameter, 5 mm grinding wheel width and thickness, and 100% concentration. The lubricating fluid in conventional flood lubricants consists of emulsifiers, mineral oil, other additives, etc, and the flow rate is 15 mL/h. KS1040 lubricating oil is used in MQL lubrication, and the discharge volume of the MQL nozzle is 60 mL/h. Oil molecules and water molecules are mixed with compressed air through the MQL system to form atomized oil-attached water droplets, and under the action of compressed air provided by the air pump, the oil-water mixture is sprayed to the grinding processing area at a certain speed through the nozzle to cool and lubricate the grinding area.

The analysis equipment includes 3D measuring laser microscope, 3D profiler, Ultra Plus field emission scanning electron microscopy (FEM), microhardness tester and dynamometer. Where the 3D measuring laser microscope is used to measure the surface roughness and observe the surface morphology. The dynamometer is used to record the changes of grinding force during the grinding process. The 3D profiler is used to obtain the 3D profile of grinding surface. The field emission scanning electron microscope is used to observe the metallographic microstructure and the grinding chip morphology. The microhardness tester is used to observe and measure the microhardness at different depths of the grinding subsurface.

3.2 Experimental material

Ni-base single crystal superalloy DD5 was used for the experiment, which has only one grain and no transverse crystal boundary perpendicular to the principal stress. Its internal atoms are arranged repeatedly and periodically in a certain order. The atoms in different crystal orientations are arranged differently, and the properties of each crystal direction are also other. So it is a typical anisotropic material and belongs to the FCC structure. It is mainly composed of matrix phase (γ phase) and intermetallic

compound (γ' phase), as shown in Fig. 4. Al and Ti elements are the main forming elements of the γ' phase, and the content of these two elements is directly determined by γ' Phase content. So, the strength and physical properties of Ni-base single crystal superalloy are mainly determined by the content of Al and Ti in the γ' Phase. γ phase especially improves the plasticity of the material, accounting for about 70% of the volume of Ni-base single crystal superalloy. Therefore, Re, Co, Cr, Mo, Al and other alloy elements are often added for strengthening γ Phase harmony γ' Phase to improve its comprehensive performance. In addition, Cr, Al and other elements in the alloy can also form a dense oxide film with air at high temperatures to cover the alloy surface and improve its corrosion resistance and oxidation resistance. In the solidification process of Ni-base single crystal superalloys, Al, Ti, Ta and other elements are segregated between dendrites, they will form when their content reaches the eutectic composition γ/γ' Eutectic structure, mainly distributed between dendrites or grain boundaries. Different casting processes and alloy compositions are adopted, γ/γ' The morphology of eutectic structure is also different, and its typical morphology is lamellar, reticular and sunflower.

Table 1
Nominal composition of DD5 (wt%)

Co	Cr	Ta	Al	W	Re	Mo	Hf	C-Ni	Ni
7.5	7.0	6.5	6.2	5.0	3.0	1.5	0.15	0.05	Bal

Table 2
Main physical properties of DD5

Hardness	Yield strength	Shrinkage	Melting point
550HV	1109MPa	13.5%	1368°C

3.3 Experimental program

A single-factor experiment for planar groove grinding was used to investigate the effects of three grinding machining methods (dry, conventional flood, and MQL) on the surface integrity of the grinding of DD5. Table 3 depicts the single-factor experiment design strategy, and the grinding wheel was grinding along the (001) crystal plane and [100] crystal direction of the DD5 material in the experiment.

Table 3
Single-factor experiment of grinding surface integrity

Experimental number	v_s (m/s)	a_p (μm)	v_f (m/min)
1	15	60	0.6
2	20	60	0.6
3	25	20	0.6
4	25	40	0.6
5	25	60	0.6
6	25	80	0.6
7	25	100	0.6
8	25	60	0.2
9	25	60	0.4
10	25	60	0.8
11	25	60	1.0
12	30	60	0.6
13	35	60	0.6

4 Analysis Of Experimental Results

4.1 Grinding force

The grinding force is a critical parameter in the grinding process. In comparison to dry grinding, it can generate an oil film in the grinding region (contact area between abrasive flank and material, and between abrasive flank and debris), lowering the friction coefficient and hence the grinding force. The effect of cooling conditions on the grinding force of DD5 under different grinding parameters was measured by a dynamometer, as shown in Fig. 5, Fig. 6, and Fig. 7.

From Fig. 5, Fig. 6, and Fig. 7, it can be obtained that in the range of experimental parameters, the magnitude of the grinding force is linearly negatively correlated with the grinding speed, and linearly positively correlated with the grinding depth and the feed rate; under different grinding parameters, the grinding force obtained by DD5 under MQL conditions is the smallest, followed by that under conventional flood conditions, and the grinding force under dry grinding conditions is the largest. As can be seen from Fig. 7, the grinding force gradually increases with the increase of feed rate, but its

transformation trend is more gentle. Compared with the other two factors, the change of feed rate has less effect on the grinding force.

When the grinding speed increases or feed rate decreases, the number of grinding grains per unit time increases, resulting in a reduction in the maximum undeformed cutting thickness of the single abrasive, thus reducing the grinding force. Compared with dry grinding, the lubricating fluid helps to form an oil film in the grinding area, reducing the friction coefficient during grinding and thus directly reducing the grinding force. Compared with conventional pouring lubrication, MQL can effectively break the air barrier caused by the high-speed rotation of the grinding wheel into the grinding area for lubrication and cooling, which can significantly reduce the grinding force during the grinding process.

4.2 Surface roughness

A LEXT OLS4100 confocal microscope was used to measure the workpiece's surface roughness, and the influence laws of each grinding parameter on the surface roughness of DD5 under different cooling conditions were plotted, as shown in Fig. 8, Fig. 9, and Fig. 10.

From Fig. 8, within the experiment settings, the surface roughness of the workpiece reduces as the grinding speed increases. The reason for this is that as the grinding speed increases, the quantity of abrasive grains involved in grinding per unit time increases, and the maximum undeformed cutting thickness decreases, which reduces the plasticity of the workpiece material and removes the lamellar chips before it can be deformed during grinding, taking away part of the grinding heat, reducing the machined surface roughness and improving the surface finish. From Fig. 9 and Fig. 10, it can be seen that the surface roughness of the workpiece increases with the rise of grinding depth or feed rate within the experimental parameters. For the reason that when the grinding depth or feed speed rises, the maximum undeformed cutting thickness of the single abrasive increases, the surface roughness Ra of the workpiece increases accordingly, and the grinding surface quality decreases.

Under different grinding process parameters, the surface roughness of DD5 obtained under MQL condition is the smallest, followed by the surface roughness obtained under conventional pouring condition, and the surface roughness obtained under dry grinding condition is the largest. This is mainly since the lubricating fluid can penetrate the grinding area to form an oil film, which reduces the friction coefficient and reduces the generation of grinding heat, thus significantly reducing the surface roughness and enhancing the surface quality of DD5. Compared with the traditional pouring lubrication, MQL can effectively break the boundary layer of air in the grinding area and enter the grinding area for lubrication and cooling. The high-pressure airflow constitutes convective heat exchange with the gas environment in the grinding area, reducing the grinding temperature. The high-pressure airflow also carries away the generated grinding chips, preventing material coating or grinding wheel clogging, etc.

4.3 Surface morphology

The surface formation mechanism of grinding process determines its surface microstructure, which will have certain effects on its machining quality, and a tiny number of micro defects may undoubtedly occur

during the process, which includes micro grooves, micro protrusions and micro-cracks, etc. A small number of grinding burns will also be generated during the grinding process. The grinding surface morphology of the DD5 material was examined using FEM under various cooling settings, as illustrated in Fig. 11.

As seen in Fig. 11, DD5 is prone to microscopic defects during the grinding process. In particular, DD5 grinding under dry environment has more significant microscopic defects with the lowest surface quality compared to Flood and MQL. To further explore the impact of cooling conditions on the surface morphology of DD5, the VHX-1000E super depth-of-field microscope was utilized to examine its surface morphology under different grinding depths, as illustrated in Fig. 12.

From Fig. 12, it can be seen that the grinding surfaces acquired with conventional flood cooling and MQL cooling are significantly better than those obtained with dry grinding under different cooling conditions and grinding depths. With the gradual rise of the grinding depth, the quality of the grinding surface gradually deteriorates and phenomena such as chip adhesion appear, and even local grinding burns appear when the grinding depth reaches 100 μm under the conditions of dry grinding and using MQL cooling. Although MQL cooling has a good lubricating effect, its cooling effect is limited. In the actual machining process, the grinding depth should be properly reduced to obtain better grinding surface quality.

To further investigate the abrasion marks of the grinding process surface and its distribution characteristics, Micromeasure 3D profiler was used to obtain the 3D profile of the grinding surface of DD5 under MQL cooling conditions, as shown in Fig. 13. Among them, the three-dimensional profile is shown on the left, the X-axis profile fitting curve is shown in the middle, and the height frequency distribution is shown on the right.

From Fig. 13, it can be seen that the variation pattern of the three-dimensional profile of the DD5 grinding surface at different grinding depths is basically the same as that of the two-dimensional grinding surface morphology. When the grinding depth is larger, deeper gullies appear in the grinding surface, the variation range of the height in the 3D profile is larger, and the probability distribution range of the grinding surface height is wider. When the grinding depth is smaller, the grinding marks in the grinding surface are wider and the distribution tends to be uniform, the variation range of the height in the 3D profile is smaller, the probability distribution range of the grinding surface height is narrower, the texture of the grinding surface is clear, and the grinding surface quality is better. The probability distribution of the grinding surface height approximately obeyed the normal distribution.

4.4 Subsurface microstructure

The Ni-base single crystal superalloy is subjected to various compound thermal and mechanical loads during the grinding process, and the material undergoes plastic deformation, resulting in various defects or damages on the surface and subsurface of the workpiece. The machined experimental workpiece was first to cut into subsurface specimens with a width of 1 mm using a CA20 low-speed wire-cut machine.

Then, the subsurface specimens were ground and polished after mounting on the mounting machine. Finally, the subsurface specimens were etched. The treated subsurface specimens were observed by FEM, as shown in Fig. 14.

As can be seen in Fig. 14, the internal microstructure of the Ni-base single crystal superalloy DD5 consists of γ phase and γ' phase, γ' equivalently embedded in γ phase, and its volume fraction is about 70%. After the grinding process with different cooling conditions, a certain thickness of the work-hardening layer and plastic deformation layer appeared on the grinding subsurface of the Ni-base single crystal superalloy DD5, where the work-hardening layer was located at the most superficial layer, followed by the plastic deformation layer, the elastic deformation layer, and the matrix. The γ phase and γ' phase in the plastic deformation layer produced distortion and plastic slip phenomena under the action of grinding process. After conventional flood cooling and MQL cooling, the thickness of the work-hardened layer on the grinding subsurface was significantly smaller than that of the work-hardened layer in dry grinding, which indicates that the use of lubricating fluid can effectively suppress the grinding work-hardening phenomenon. This is because the lubricating fluid helps to form an oil film in the grinding area, which reduces the friction coefficient and friction force, thus reducing the degree of grinding hardening.

4.5 Microhardness

The grinding surface undergoes violent plastic deformation, the surface lattice of the workpiece is distorted, the surface grains are broken, elongated and distorted, hindering their deformation, improving the strength and hardness of the metal, and the material is strengthened by the deformation. At the same time, the grinding surface also undergoes thermal softening effect in high-temperature environment. Under this dual effect of weakening and strengthening, it may cause the machined surface to work harden and may also reduce the hardness of the machined surface. Microhardness is one of the most important means of studying the microstructural properties of metallic materials. It is obtained by applying a small load on the surface to be measured using a microhardness indenter to produce a micro indentation, which is calculated by determining the diagonal length of the micro indentation. Since the load applied by Vickers hardness is smooth and has no impact on the sample, the microhardness experiment in this paper adopts the Vickers hardness method and uses a diamond orthotropic indenter for loading, with the angle between the two opposite faces at the top of the vertebrae being 136°, and the four faces at the top of the indenter intersecting at a point, with the length of any intersection line between the opposite faces not greater than 1 μm.

A digital display Vickers microhardness tester was used to examine the subsurface microhardness of the Ni-base single crystal superalloy DD5 under three grinding processing methods (grinding speed of 25 m/s, grinding depth of 60 μm, and feed rate of 0.6 m/min) and to obtain micro indentations at different measurement positions. The microscopic indentations at different measurement positions were obtained using the step method, as shown in Fig. 15. With the grinding surface as the starting point, the diamond orthotropic indenter was slowly pressed into the measured sample surface and moved toward the substrate, and the load was applied at an interval of 5 μm, with a load size of 0.245 N and a holding time of 8 s. A total of 30 times were loaded, and the measurement range was from 5 to 150 μm below the

grinding surface. after obtaining the two diagonal lengths of the micro indentation, the average value was taken as the length of the micro indentation d. The microhardness HV at different measurement locations was calculated according to Eq. (1).

$$HV = \frac{189089.43P}{d^2} 1$$

Where: d is the length of the diagonal of the microscopic indentation (μm); P is the load applied to the experiment (N).

Based on the obtained microhardness values at different measurement locations on the ground subsurface, the curves of DD5 subsurface microhardness variation patterns under different cooling conditions were plotted, as shown in Fig. 16, Fig. 17, and Fig. 18.

As can be seen in Fig. 16, Fig. 17, and Fig. 18, the subsurface microhardness under the three grinding processing methods (dry, flood, and MQL) of the Ni-base single crystal superalloy DD5 has a similar variation pattern. The subsurface microhardness of the three grinding methods decreases sharply with increasing distance from the grinding surface from 5 μm to 15 μm, with the microhardness of dry grinding being the largest, followed by that of using conventional flood, and the microhardness of cooling with MQL being the smallest. At a distance of 20 μm-150 μm from the grinding surface (material substrate position), the grinding process of the three grinding processing methods had less influence on their subsurface microhardness, and the microhardness of all three fluctuated around 540 HV. Based on the above conclusions, it can be concluded that the microhardness of the grinding metamorphic layer is greater than the microhardness of the material matrix, which indicates that the grinding process of the Ni-base single-crystal superalloy DD5 prompted the strengthening of its ground surface organization.

4.6 Chip morphology

The microscopic morphology of grinding chips can represent the removal mechanism of material grinding, while the size and shape of grinding chips can reflect the plastic deformation of material and the form of removal during the grinding process. The formation of grinding chips marks the realization of the grinding process. Studying the formation process of grinding chips of Ni-base single crystal superalloys can help reveal the grinding and removal mechanism of Ni-base single crystal superalloys more deeply and offer a theoretical foundation for analyzing the grinding process and grinding surface quality. As illustrated in Fig. 19, a swarf collecting box was put on the grinding machine table to collect the swarf created during the grinding experiment (under varied cooling settings), and the surface morphology was studied using the Ultra Plus field emission scanning electron microscope.

As shown in Fig. 19, under different cooling conditions, DD5 mainly produces serrated chips, which mainly have two typical surfaces: contact surface and free surface. The side inclined to the rake face of abrasive particles is called the contact surface, which is mainly smooth and flat, and there are traces of abrasive particles sliding on the inner surface of abrasive chips. The opposite side is known as the free

surface; unlike the contact surface, the free surface is primarily exhibited as a lamellar structure. The reason for this is that when the stress on the shear surface surpasses the strength limit of the material in the process of shaping and deforming the material under the action of the abrasive grains, the abrasive chips are sheared to form lamellar chips. During the grinding process, the interaction between the abrasive grains and the workpiece generates a large amount of grinding heat. Meanwhile, because the abrasive grains generally have a negative front angle, the grinding will intensify the material deformation and generate high temperature. As a large amount of grinding heat is not released in time, the material is more likely to undergo adiabatic shearing to form serrated chips. Ni-base single crystal superalloy has high strength, thermal strength and low thermal conductivity, and is a typical difficult-to-machine material, so the grinding temperature generated during grinding is difficult to conduct out, and the degree of adiabatic shear is more obvious, and the shear slip phenomenon is easy to occur.

At the same time, a phenomenon can be found that the chip morphology of DD5 in MQL or conventional flood environment is more regular than that in dry environmental conditions. The degree of sawing of the chips in the flood or MQL environment is obvious, and the chip formation frequency fluctuates less and the chip formation is stable. In contrast, the chip morphology in dry environment is less regular, the chip formation frequency fluctuates more, and the chip formation is not stable. This is because the degree of work hardening of DD5 in dry environment is greater, and the microhardness of the material increases, which makes it difficult to form chips. Conventional flood lubrication and MQL help to reduce the microhardness of the material and improve the removal rate of the material.

The individual grinding chips (in dry, flood, and MQL environments) were observed for different grinding wheel linear speeds, and Fig. 20 was obtained.

As shown in Fig. 20, under different cooling conditions, the frequency of serrated unit formation and the degree of serration on the free surface of the grinding chips increased with the increase of grinding speed. When the grinding wheel linear speed was 15 m/s and 25 m/s, the frequency of formation of serrated units on the free surface of the grinding chips and the degree of serration were lower. When the grinding speed is 35m/s, the frequency of formation of serrated units and the degree of serration on the surface of the grinding chip is the highest, and the size of the grinding chip is larger at this time. This is because. With the increasing speed, the number of abrasive grains involved in the grinding process per unit time increases, the temperature in the deformation zone of the material rises sharply, and the transient high temperature generated by the grinding process promotes its thermoplastic instability, making the material more susceptible to adiabatic shear slip, generating more slip elements per unit time and increasing the degree of swarf serration.

5 Conclusion

The following conclusions can be drawn from the experimental study of the surface integrity of the Ni-base single crystal superalloy DD5 grinding under different cooling conditions.

1. The grinding surface roughness and grinding force of the Ni-base single crystal superalloy DD5 obtained under different cooling conditions were in the order of MQL, conventional flood, and dry grinding from low to high.
2. When the grinding depth is large, the grinding surface quality is poor, with deep scratches and grooves. Under the conditions of dry grinding and using MQL cooling, local grinding burns appear when the grinding depth reaches 100μm. The grinding depth should be reduced appropriately to obtain better grinding surface quality in the actual machining process.
3. The organization of the ground surface layer of the Ni-base single crystal superalloy DD5 was strengthened. After conventional flood cooling and MQL cooling, the thickness of the work-hardened layer on the ground subsurface was significantly smaller than that of the dry grinding. The microhardness of DD5 subsurface decreases sharply with the increase of distance from the grinding surface when it is 5 ~ 15 μm from the grinding surface; when it is 20 ~ 150 μm from the grinding surface, the microhardness of DD5 subsurface remains balanced and fluctuates around 540 HV.
4. Conventional flood lubrication and MQL help to reduce the microhardness of the material and improve the removal rate of the material. The degree of abrasive chip serration of DD5 in flood or MQL environment is obvious, its abrasive chip formation frequency fluctuates less and the chip formation is stable. In contrast, the degree of chip morphology regularization in dry environment is lower, its chip formation frequency fluctuates more, and the chip formation is not stable.

Declarations

Funding This work was supported by the National Natural Science Foundation of China (NO. U1908230&51775100), the Science and Technology Research Project of the Educational Department of Liaoning Province (NO. LJKZ0384&L2017LQN024), the Talent Scientific Research Fund of LNPU (NO. 2021XJJL-007).

Competing interests The authors have no relevant financial or non-financial interests to disclose.

Availability of data and material All data and materials used to produce the results in this article can be obtained upon request from the corresponding author.

Code availability Not applicable.

Ethics approval The authors declare that there is no ethical issue applied to this article.

Consent to participate The authors declare that all authors have read and approved to submit this manuscript to IJAMT.

Consent for publication The authors declare that all authors agree to sign the transfer of copyright for the publisher to publish this article upon on acceptance.

Authors' contributions Ming Cai: Writing - original draft, software, investigation, visualization. Tao Zhu: Writing - original draft, review and editing, conceptualization, funding, visualization. Xingjun Gao:

Conceptualization, methodology, formal analysis. Yongfei Yan: Supervision, investigation, methodology. Ning Yu: Data curation, formal analysis. Lei Zeng: Data curation, formal analysis.

References

1. Dai CW, Ding WF, Xu JH, Fu YC, Yu TY (2017) Influence of grain wear on material removal behavior during grinding nickel-based superalloy with a single diamond grain. Int J Mach Tools Manuf 113:49–58. https://doi.org/10.1016/j.ijmachtools.2016.12.001
2. Zhou YG, Gong YD, Zhu ZX, Gao Q, Wen XL (2016) Modelling and optimization of surface roughness from micro-grinding of nickel-based single crystal superalloy using the response surface methodology and genetic algorithm. Int J Adv Manuf Technol 85(9–12):2607–2622. https://doi.org/10.1007/s00170-015-8121-z
3. Miao Q, Ding WF, Kuang W, Yang C (2020) Comparison on grindability and surface integrity in creep feed grinding of gh4169, k403, dz408 and dd6 nickel-based superalloys. J Manuf Process 49:175–186. https://doi.org/10.1016/j.jmapro.2019.11.027
4. Cai M, Gong YD, Sun Y, Qu SS, Liu Y, Yang YY (2019) Experimental study on grinding surface properties of nickel-based single crystal superalloy dd5. Int J Adv Manuf Technol 101:71–85. https://doi.org/10.1007/s00170-018-2839-3
5. Cai M, Gong YD, Qu SS, Yang YY (2019) Experiment of Grinding Surface Quality and Subsurface Microstructure for Nickel-Based Single Crystal Superalloy. J Northeast Univ 40(3):386–391. https://doi.org/10.12068 /j.issn.1005-3026.2019.03.016
6. Ding WF, Dai CW, Yu TY, Xu JH, Fu YC (2017) Grinding performance of textured monolayer CBN wheels: undeformed chip thickness nonuniformity modeling and ground surface topography prediction. Int J Mach Tools Manuf 122:66–80. https://doi.org/10.1016/j.ijmachtools.2017.05.006
7. Li BK, Ding WF, Li M, Zhang X (2021) Tool wear behavior of alumina abrasive wheels during grinding FGH96 powder metallurgy nickel-based superalloy. Procedia CIRP 101:182–185. https://doi.org/10.1016/j.procir.2020.04.161
8. Li BK, Dai CW, Ding WF, Yang CY, Li CH, Kulik O, Shumyacher V (2020) Prediction on grinding force during grinding powder metallurgy nickel-based superalloy FGH96 with electroplated CBN abrasive wheel. Chin J Aeronaut 34(8):65–74. https://doi.org/10.1016/j.cja.2020.05.002
9. Li M, Yin JF, Che LB, Ding WF, Xu JH (2021) Influence of alumina abrasive tool wear on ground surface characteristics and corrosion properties of K444 nickel-based superalloy. Chin J Aeronaut. https://doi.org/10.1016/j.cja.2021.06.008
10. Ruzzi R, Paiva R, Silva LRRD, Abrão AM, Brandão LC, Silva RBD (2021) Comprehensive study on Inconel 718 surface topography after grinding. Tribol Int 158:106919. https://doi.org/10.1016/j.triboint.2021.106919
11. Zhao Z, Qian N, Ding WF, Wang Y, Fu YC (2020) Profile grinding of DZ125 nickel-based superalloy: grinding heat, temperature field, and surface quality. J Manuf Process 57:10–22.

https://doi.org/10.1016/j.jmapro.2020.06.022

12. Gong YD, Zhou YG, Wen XL, Cheng J, Sun Y (2017) Experimental study on micro-grinding force and subsurface microstructure of nickel-based single crystal superalloy in micro grinding. J Mech Sci Technol 31:3397–3410. https://doi.org/10.1007/s12206-017-0629-8
13. Tian L, Fu YC, Xu JH, Li H, Ding WF (2015) The influence of speed on material removal mechanism in high speed grinding with single grit. Int J Mach Tools Manuf 89:192–201. https://doi.org/10.1016/j.ijmachtools.2014.11.010
14. Öpöz TT, Chen X (2012) Experimental investigation of material removal mechanism in single grit grinding. Int J Mach Tools Manuf 63:32–40. https://doi.org/10.1016/j.ijmachtools.2012.07.010
15. Öpöz TT, Chen X (2014) Experimental study on single grit grinding of Inconel 718. Proc Int Mach Eng Part B: J Eng Manch 229(5):1–14. https://doi.org/10.1177/0954405414531114
16. Öpöz (2013) Comparison of material removal characteristics in single and multiple cutting edge scratches. Adv Mater Res, 797: 189–195.https://doi.org/10.4028/www.scientific.net/AMR.797.189.
17. Virdi RL, Chatha SS, Singh H (2021) Experimental investigations on the tribological and lubrication behaviour of minimum quantity lubrication technique in grinding of Inconel 718 alloy. Tribol Int 153:106581. https://doi.org/10.1016/j.triboint.2020.106581
18. Yazid MZA, CheHaron CH, Ghani JA, Ibrahim GA, Said AYM (2011) Surface integrity of Inconel 718 when finish turning with PVD coated carbide tool under MQL. Proc Eng 19:396–401. https://doi.org/10.1016/j.proeng.2011.11.131
19. He AD, Ye BY, Qin MY, Xu LY, Liang LD (2014) Effect of micro lubrication on cutting residual stress. J Hunan Univ 42(10):48–53. https://doi.org/10.16339/j.cnki.hdxbzkb.2015.10.008
20. Li Q, Gong YD, Cai M, Li MJ (2017) Research on surface integrity in milling Inconel718 superalloy. Int J Adv Manuf Technol 92(1):1449–1463. https://doi.org/10.1007/s00170-017-0080-0
21. Silva LRD, Bianchi EC, Fusse RY, Catai RE, Franc-a TV, Aguiar PR (2007) Analysis of surface integrity for minimum quantity lubricant—MQL in grinding. Int J Mach Tools Manuf 47(2):412–418. https://doi.org/10.1016/j.ijmachtools.2006.03.015
22. Balan ASS, Vijayaraghavan R, Krishnamurthy P, Kuppan R, Oyyaravelu (2016) An experimental assessment on the performance of different lubrication techniques in grinding of Inconel 751. J Adv Res 7(5):709–718. https://doi.org/10.1016/j.jare.2016.08.002
23. Khanna N, Agrawal C, Pimenov DY, Singla AK, Machado AR, Silva LRRD, Gupta MK, Sarikaya M, Grzegorz M, Krolczyk (2021) Review on design and development of cryogenic machining setups for heat resistant alloys and composites. J Manuf Process 68(A):398–422. https://doi.org/10.1016/j.jmapro.2021.05.053
24. Krolczyk GM, Maruda RW, Krolczyk JB, Wojciechowski S, Mia M, Nieslony P, Budzik G (2019) Ecological trends in machining as a key factor in sustainable production-A review. J Clean Prod 218:601–615. https://doi.org/10.1016/j.jclepro.2019.02.017
25. Bhuyan M, Sarmah A, Gajrani KK, Pandey A, Thulkar TG, Sankar MR (2018) State of Art on Minimum Quantity Lubrication in Grinding Process. Mater Today: Process 5(9):19638–19647.

https://doi.org/10.1016/j.matpr.2018.06.326

26. Jia DZ, Zhang NQ, Liu B, Zhou ZM, Wang XP, Zhang YB, Mao C, Li CH (2021) Particle size distribution characteristics of electrostatic minimum quantity lubrication and grinding surface quality evaluation. Diam Abras Eng 3(41):89–95. https://doi.org/10.13394/j.cnki.jgszz.2021.3.0013
27. Gong YD, Zhang WJ, Cai M, Zhou XX (2020) Experimental Study on the Grinding Metamorphic Layer of Nickel-based Single Crystal Superalloy. J Northeast Univ 41(6):846–851. https://doi.org/10.12068/j.issn.1005-3026.2020.06.015
28. Wang YG, Li CH, Zhang YB, Li BK, Yang M (2016) Experimental evaluation of the lubrication properties of the wheel/workpiece interface in minimum quantity lubrication (MQL) grinding using different types of vegetable oils. J Clean Prod 127:487–499. https://doi.org/10.1016/j.triboint.2016.03.023
29. Guo SM, Li CH, Zhang YB, Wang YG, Li BK, Yang M, Zhang XP, Liu GT (2017) Experimental evaluation of the lubrication performance of mixtures of castor oil with other vegetable oils in MQL grinding of nickel-based alloy. J Clean Prod 140:1060–1076. https://doi.org/10.1016/j.jclepro.2016.10.073
30. Yuan SM, Zhu GY, Wang L (2017) Recent Progress on Lubricant Characteristics of Minimum Quantity Lubrication (MQL) Technology in Green Cutting. Chin J Mech Eng 53(17):131–140. https://doi.org/10.3901/JME.2017.17.131

Figures

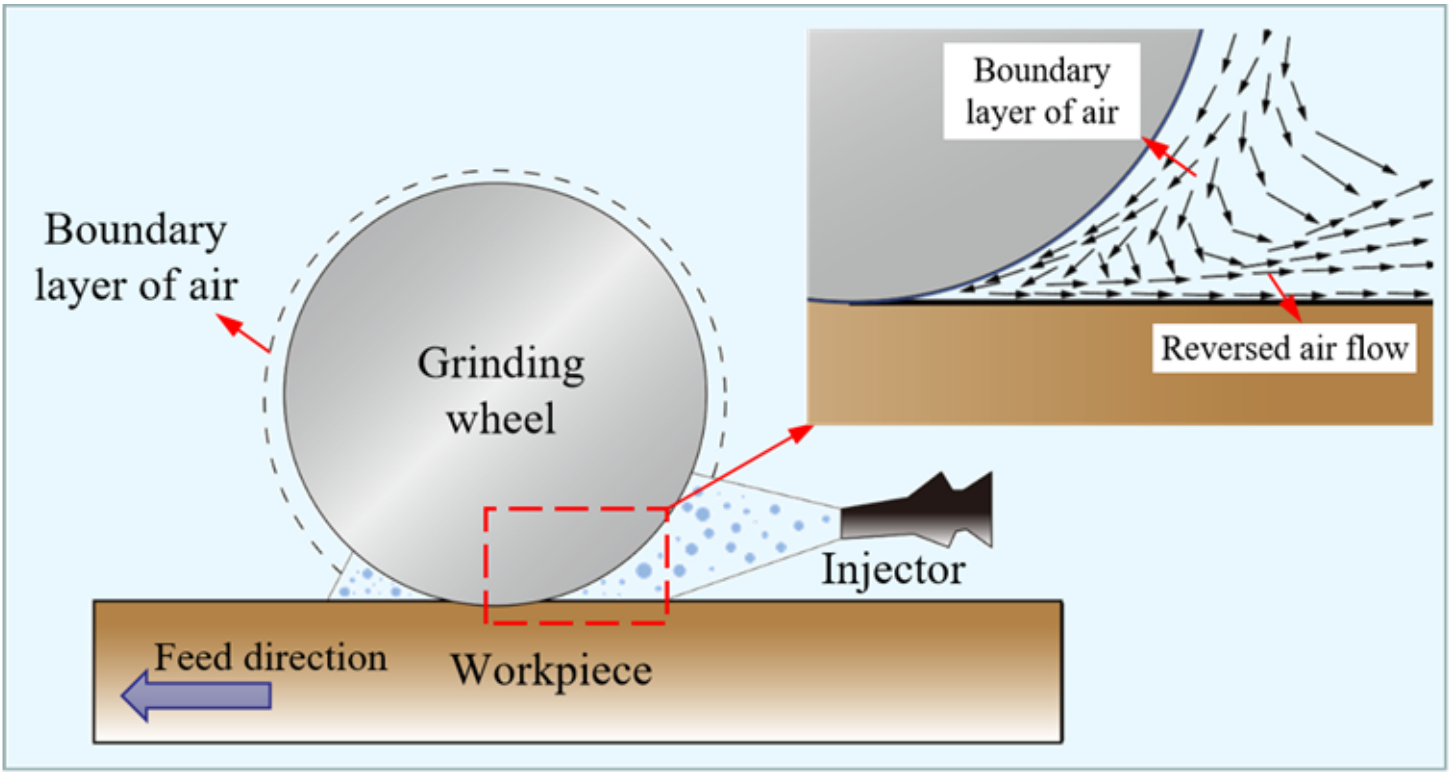

Figure 1

Schematic diagram of MQL

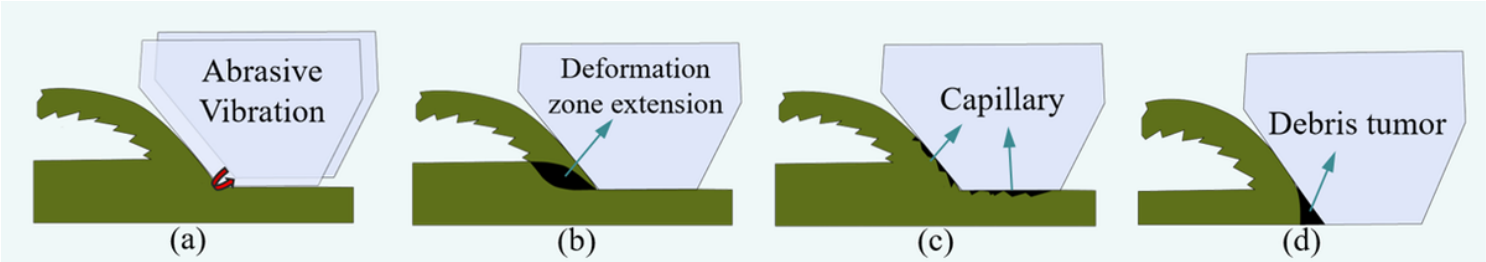

Figure 2

Permeation mechanism of lubricating fluid

Figure 3

Experimental equipment

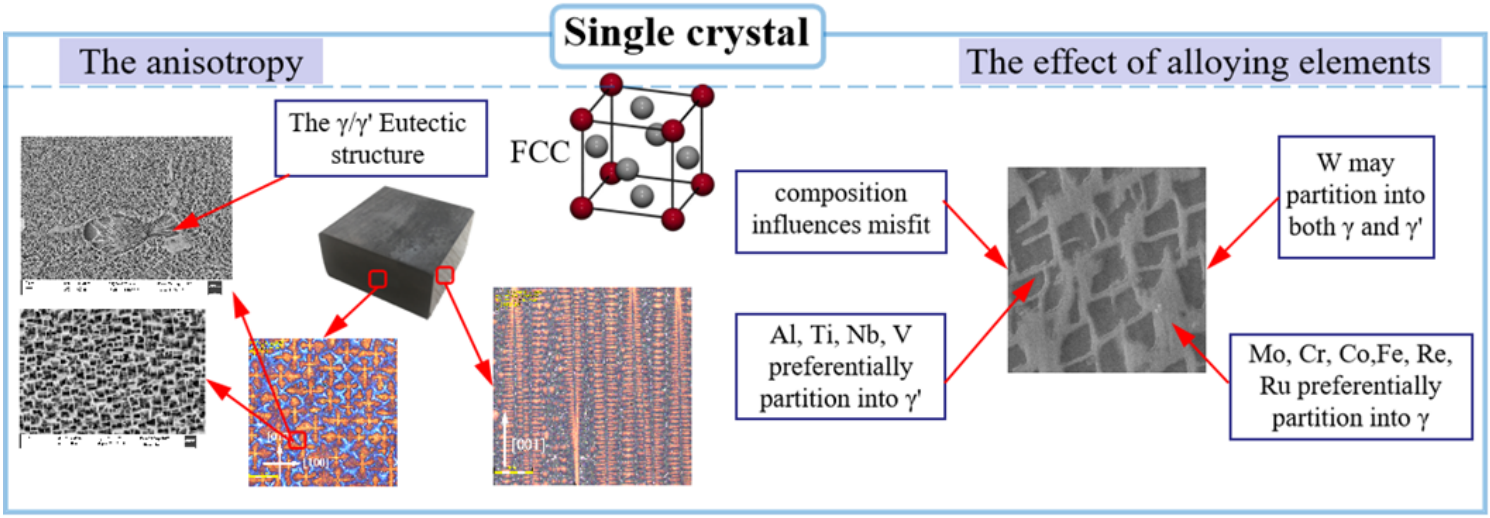

Figure 4

The microstructure of DD5

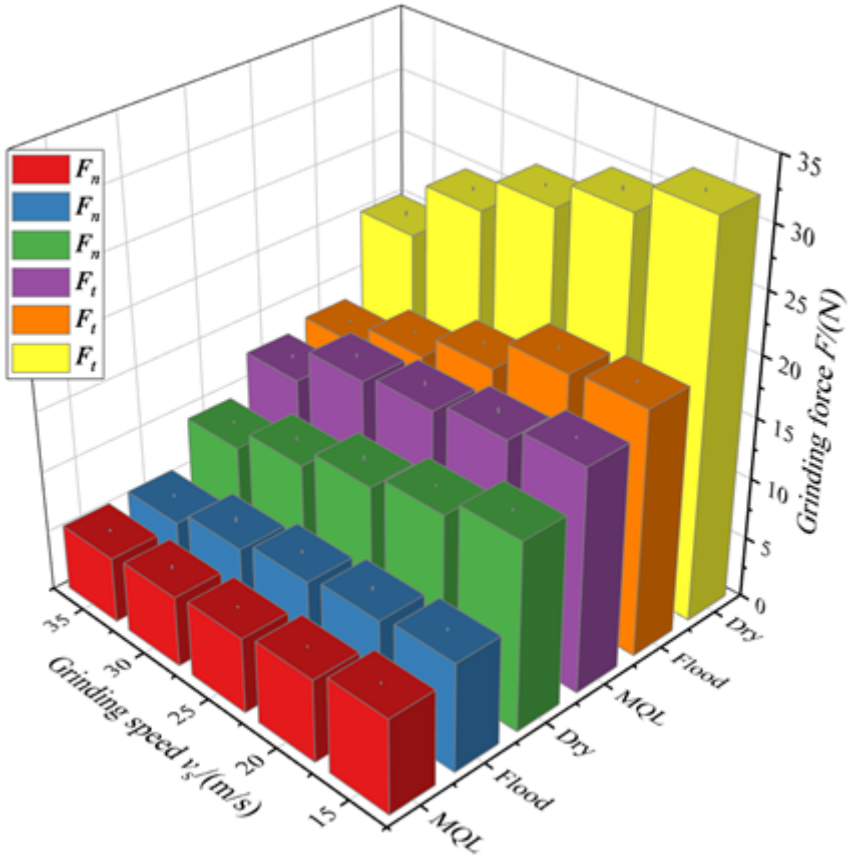

Figure 5

Impact of cooling conditions on the grinding force at different grinding speeds

Figure 6

Impact of cooling conditions on the grinding force at different grinding depths

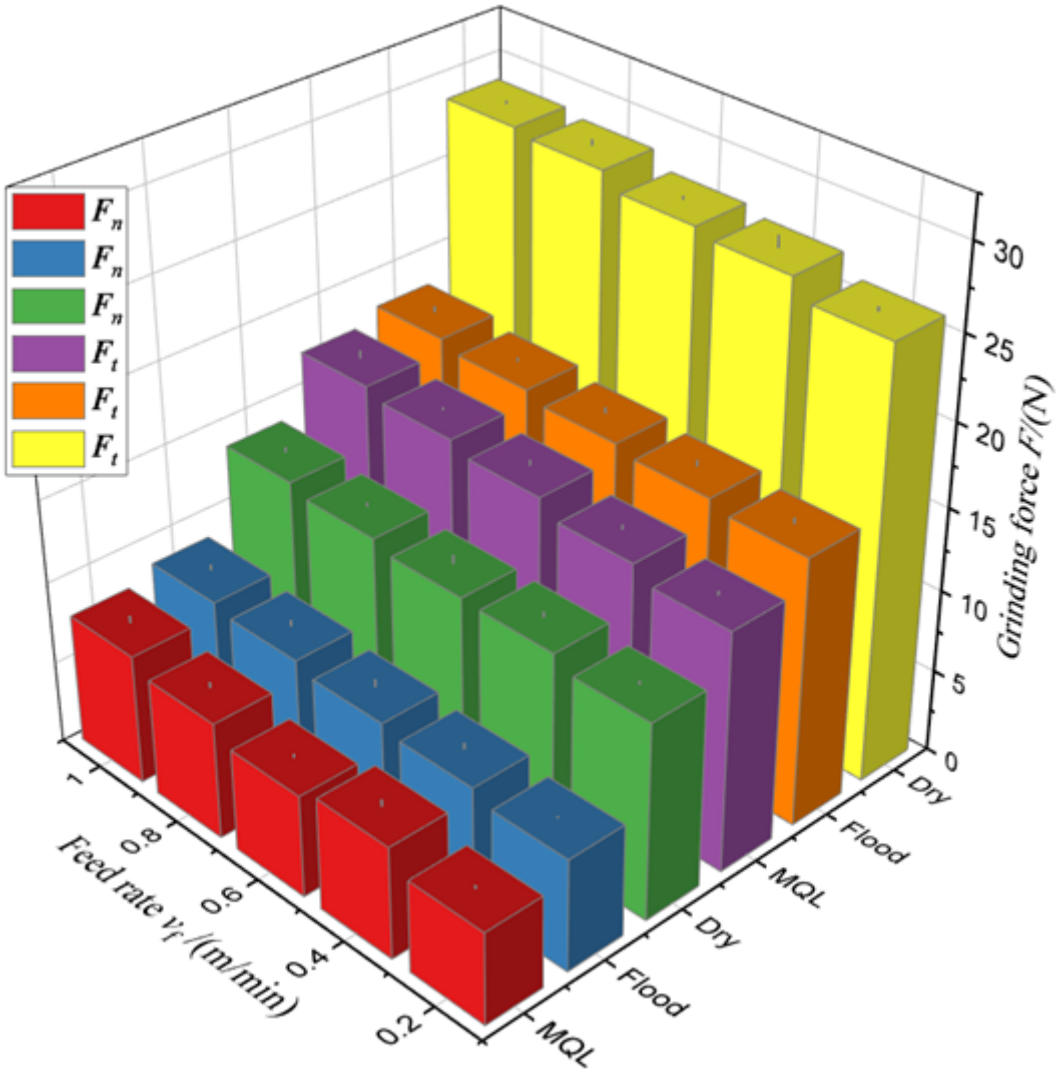

Figure 7

Impact of cooling conditions on grinding force at different feed rates

Figure 8

Impact of grinding speed on surface roughness under different cooling conditions

Figure 9

Impact of grinding depth on surface roughness under different cooling conditions

Figure 10

Impact of feed rate on surface roughness under different cooling conditions

Figure 11

Grinding surface morphology under different cooling conditions

Figure 12

Effect of cooling conditions on the surface morphology at different grinding depths

Figure 13

Grinding surface three-dimensional profile under different grinding depths

Figure 14

Microstructure of grinding subsurface under different cooling conditions

Figure 15

Microhardness measurement with step method

Figure 16

Microhardness of grinding subsurface under dry condition

Figure 17

Microhardness of grinding subsurface under conventional flood condition

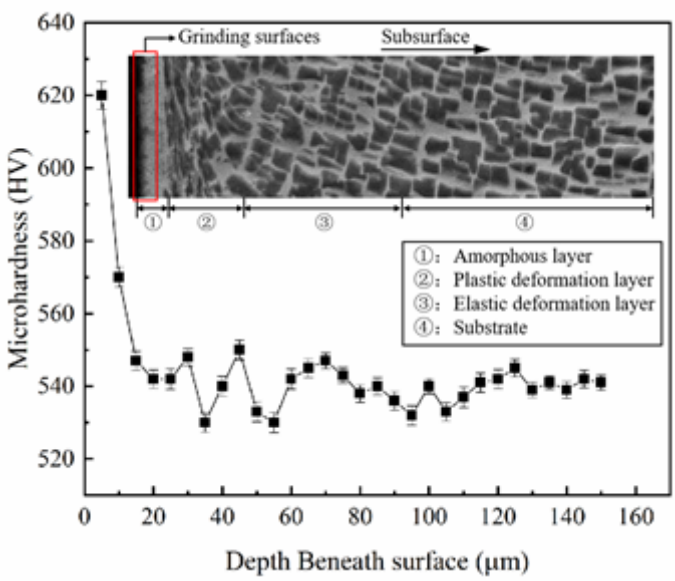

Figure 18

Microhardness of grinding subsurface under MQL condition

Figure 19

Chip morphology under different cooling conditions

Figure 20

Effect of grinding speed on chip morphology under different cooling conditions